

Eduard A. Lysenkov<sup>1\*</sup>, Oleksandr V. Striutskyi<sup>2</sup>

<sup>1</sup>Petro Mohyla Black Sea National University, 10, 68 Desantrnykiv St., Mykolaiv, Ukraine, 54003

<sup>2</sup>National Academy of Sciences of Ukraine, Institute of Macromolecular Chemistry, 48, Kharkivske Highway, Kyiv, Ukraine, 02160

\*Corresponding author. E-mail: ealysenkov@ukr.net

Received (Otrzymano) 5.05.2023

## INFLUENCE OF FILLER INTRODUCTION METHOD ON STRUCTURE AND PROPERTIES OF POLYMER COMPOSITES BASED ON POLYURETHANE AND SILVER NANOPARTICLES

Polymer nanocomposites based on segmented polyurethane and silver nanoparticles (AgNPs) were synthesized using different methods of nanoparticle introduction. The dependence of their structure, thermophysical and antimicrobial properties on the method of introducing AgNPs was studied. It was established that the method of introduction affects both the spatial distribution of the filler particles and the final properties of the material. The introduction of AgNPs by the ultrasonic dispersion method leads to inhibition of the growth of the crystalline phase, which is associated with the formation of aggregates from AgNPs of small size, which have a large polymer-filler interaction surface. It is shown that the introducing AgNPs from a colloidal solution leads to an increase in the degree of crystallinity of the polymer matrix, which is a consequence of the nucleation effect of nanosized silver particles on the formation of the crystalline phase. It was established that the method of introducing nanoparticles does not affect their final antimicrobial properties. Owing to their unique characteristics, synthesized nanocomposite films can be promising for use as antimicrobial coatings.

**Keywords:** polymer nanocomposites, silver nanoparticles, polyurethanes, structure, antimicrobial properties, thermophysical properties

### INTRODUCTION

Polymeric composite materials that contain nanoparticles of various nature have remained among the most interesting materials to study during the last two decades. The interest in such materials is explained, first of all, by their unique properties and operational characteristics. Depending on the choice of polymer matrix and nanofiller, it is possible to obtain a material with the required properties [1].

The method of their preparation has a significant influence on the final properties of nanocomposite materials. The most common manufacturing methods for introducing nanoparticles into the polymer matrix are extrusion [2, 3], ultrasonic dispersion [4, 5], sol-gel synthesis [6, 7] and *in situ* polymerization [8, 9]. Each method has its advantages and disadvantages and can be used for a specific combination of polymer and nanofiller.

One of the promising areas of modern polymer materials science is the development of new antimicrobial materials [10]. The most active antimicrobial filler is silver nanoparticles (AgNPs), which exhibit high inhibitory activity against most bacteria and fungi [11, 12]. Nanocomposite materials containing AgNPs can retain their antimicrobial activity for a long period of time. However, the method of preparation of polymer-AgNP

systems significantly affects their final physicochemical properties and antimicrobial characteristics.

The methods of obtaining polymer nanocomposites that contain AgNPs can be divided into two groups: one-step and two-step methods [13]. In the one-step method, the silver precursor and polymer, which serves as a stabilizer for the silver nanoparticles, share the same solvent. Selective solvents must be used in this method so that both the precursor and polymer can be dissolved.

Ljutakov et al. proposed a simple one-step procedure for the *in situ* preparation of silver nanoparticles in polymer thin films [14]. The nanoparticles were prepared by the reaction of N-methyl pyrrolidone with silver salt in a semi-dry polymer film. The antimicrobial properties of AgNPs/PMMA films were found to be dependent on the concentration of NPs, their size and distribution. The authors concluded that the direct synthesis of NPs in polymer has several advantages; it avoids time-consuming AgNP mixing with the polymer matrix, and uniform silver distribution in polymer films is achieved without the necessity for additional stabilization. Nevertheless, this method also has its disadvantages, the main of which is the limited number of polymers that can be used as the matrix.

In the two-step method of nanocomposite preparation, polymer matrices or AgNPs are synthesized separately, and then the two components connect. For example, in the first step Demchenko et al. synthesized a polymer matrix based on pectin and polyethyleneimine [15]. Then the thermochemical reduction of  $\text{Ag}^+$  ions in the polymer films was performed by heating up them to 100-160°C for 5-30 min. In this way, it was possible to obtain uniformly distributed silver nanoparticles in the polymer matrix. In work [16], the authors first synthesized stabilized AgNPs, and then introduced them into the molten polymer matrix of polyethylene oxide. A nanocomposite with 1% AgNPs exhibits significant activity for *Klebsiella* (the zone of inhibition is 19 mm) and material with 2% AgNPs exhibits significant activity for *S. aureus* (the zone of inhibition is 22 mm). However, during the process of mixing with polymer, due to the high viscosity of molten polymers or the polymer solution, AgNPs tend to aggregate and lose their antimicrobial properties [17]. To solve this problem, the *in situ* method of monomer polymerization of in the presence of AgNPs is used [9].

Demchenko et al. studied the influence of preparation methods on the structure and properties of antimicrobial polymer materials containing AgNPs [18]. Two methods were used to prepare polymer nanocomposites based on polylactic acid and silver nanoparticles: the mechanical method and the *in situ* method. It was established that the preparation method affects the average size of the silver nanoparticles. Thus, when using the mechanical method of preparation, silver nanoparticles with a size of 16 nm were distributed in the polymer matrix, and in the case of the *in situ* method, the size of the nanoparticles was about 4 nm. The method of preparation of the polymer-silver systems also affects their antimicrobial properties. It was shown that the materials prepared by the *in situ* method exhibit high antimicrobial activity against gram-positive and gram-negative bacteria, as well as fungi, while no antimicrobial activity was observed for the materials prepared by the mechanical method. Nonetheless, such an effect may be a consequence of the different size of the nanoparticles.

The disadvantage of the mechanical method of introduction is the uncontrolled aggregation of filler particles because the NPs were previously synthesized without stabilization. The *in situ* method of AgNP formation in a polymer matrix ensures their high surface stability and reproducibility. However, the disadvantage of the method is the necessity to use hazardous and expensive reagents, as well as the presence of their traces in AgNPs and resulting composite materials.

Today, there is no single universal method of preparing materials based on nanosilver and a polymer matrix. From the above review, it can be seen that various methods of preparing polymer nanocomposites containing silver nanoparticles lead to different properties of the obtained materials. Considering the advantages and disadvantages of the considered methods, we studied

the structure and properties of polymer systems based on polyurethanes and stabilized AgNPs prepared by the two-step method. In this case, the nanoparticles were synthesized separately and introduced into the polymer matrix solution using ultrasonic dispersion of the powder and from the colloidal solution with the subsequent removal of solvents.

## EXPERIMENTAL PART

### Materials

2-sulfobenzoic acid cyclic anhydride (Merck,  $\geq 95\%$ ), 1-methylimidazole (Merck, 99%),  $\text{AgNO}_3$  (Pharm.), trisodium citrate ( $\text{C}_6\text{H}_5\text{O}_7\text{Na}_3$ , Pharm.), toluene diisocyanate (Merck, mixture of 2,4- and 2,6-isomers in a mass ratio of 4:1) and 1,4-phenylenediamine (Merck, 98%) were used without additional purification; hyperbranched aliphatic oligoester polyol Boltorn<sup>®</sup>H30 ("Perstorp" Sweden) MM 3500 (equivalent MM of the oligomer by hydroxyl groups, determined by the acylation method, is 117 g/eq) was purified by reprecipitation from dimethylformamide (DMF) into ether, followed by drying in vacuum (1-3 mmHg) at a temperature of 25-30°C for 6 hours; polytetramethylene glycol (PTMG) MM 1000 g/mol was vacuumed at a residual pressure of 1-3 mmHg at a temperature of 70-80°C for 6 hours; DMF was distilled at a residual pressure of 1-3 mmHg, and ethanol and diethyl ether were used without distillation.

The synthesis of AgNPs was carried out by the reduction of silver ions in  $\text{AgNO}_3$  with trisodium citrate [19] in the presence of hyperbranched oligomeric ionic liquid (HB-OIL), proposed by us, as their surface stabilizer. HB-OIL was obtained according to our previously developed method [20] by the exhaustive acylation of third-generation oligoester polyol (containing 32 terminal aliphatic primary hydroxyl groups) with cyclic 2-sulfobenzoic anhydride and subsequent neutralization of the resulting reaction product with N-methylimidazole. AgNPs were obtained by boiling 0.125 g of  $\text{AgNO}_3$  and 0.731 g of  $\text{C}_6\text{H}_5\text{O}_7\text{Na}_3$  in the presence of 0.941 g of HB-OIL in 60 ml of water under reflux for 1 h. The resulting solution was evaporated, the precipitate was evacuated, washed with ethanol and dried at a residual pressure of 1-3 mmHg at 75-80°C. The product yield was 0.868 g. Characteristic signals on the FTIR spectrum for this product are observed at the following frequencies: 660, 735, 762, 802, 841, 879, 906, 1020, 1040, 1053, 1080, 1128, 1138, 1178, 1234, 1265, 1304, 1360, 1393, 1418, 1439, 1475, 1575, 1649, 1718, 2300-3700 (broadened signals of weak intensity)  $\text{cm}^{-1}$ . The synthesized product is a brown powder soluble in water and insoluble in organic solvents. The synthesized product has the designation AgNPs(1:3), which reflects the ratio of silver ions and HB-OIL ionic groups in the initial reaction mixture, respectively.

According to a similar method, NPs were synthesized with a ratio of silver ions and HB-OIL ionic

groups in the initial reaction mixture equal to 1:9 with the corresponding designation AgNPs(1:9). At the same time, silver ions were reduced in a composition of 0.044 g of AgNO<sub>3</sub> using 0.268 g of C<sub>6</sub>H<sub>5</sub>O<sub>7</sub>Na<sub>3</sub> in the presence of 1.000 g of HB-OIL. The product yield was 0.985 g. Characteristic signals on the FTIR spectrum for this product are observed at the following frequencies: 660, 735, 762, 802, 847, 878, 889, 1020, 1040, 1082, 1138, 1176, 1232, 1258, 1283, 1308, 1337, 1394, 1418, 1441, 1472, 1566, 1574, 1720, 2300-3700 (broadened signals of weak intensity) cm<sup>-1</sup>. The obtained product is a brown powder soluble in water and insoluble in organic solvents.

### Preparation of nanocomposite polymer materials PU-AgNPs

The starting polyurethane (PU) to obtain the nanocomposites was synthesized in two stages. At the first stage, an isocyanate prepolymer was obtained by the PTMG reaction with a two-fold molar excess of toluene diisocyanate by weight at 80°C in a stream of dry nitrogen. The reaction was controlled by the content of isocyanate groups by the titrimetric method. At the second stage, the final isocyanate groups of the obtained prepolymer were treated with 1,4-phenylenediamine at a ratio of NCO:NH<sub>2</sub> = 1:1 in a 10 % solution in DMF until complete consumption of the isocyanate groups according to FTIR spectroscopy. PU was used as a 10% solution in DMF in the preparation of the composites with AgNPs.

Nanocomposite polymer materials PU-AgNPs with a content of 2 wt.% AgNPs were received in two ways.

The first method of obtaining the nanocomposites was based on the ultrasonic dispersion of AgNPs in a 10% PU solution in DMF, followed by evaporation of the solvent and vacuuming of the obtained film materials (residual pressure 3-5 mmHg) at 60-70°C for 4 hours. The designations PU-AgNPs(1:3)D and PU-AgNPs(1:9)D were assigned to the nanocomposite polymer materials obtained by this method using AgNPs (1:3) and AgNPs (1:9).

The second method of obtaining nanocomposites consisted in mixing a solution of PU in DMF with an aqueous solution of AgNPs and subsequent evaporation of the mixtures at a temperature of 70-80°C and vacuuming the resulting film materials (residual pressure 3-5 mmHg) at 60-70°C for 4 hours. At the same time, the volume ratio of DMF:water was 4:1, respectively. Nanocomposite polymer materials of this type based on AgNPs (1:3) and AgNPs (1:9) have the designations PU-AgNPs(1:3)S and PU-AgNPs(1:9)S, respectively.

### Research methods

Fourier-transform infrared (FTIR) spectra were taken utilizing a spectrometer "TENSOR 37" (Bruker, Germany) in the spectral range of 600-4000 cm<sup>-1</sup>.

The structure of the obtained samples was investigated by the method of wide-angle X-ray diffraction on an XRD-7000 diffractometer (Shimadzu, Japan), using CuK $\alpha$  radiation ( $\lambda = 1.54 \text{ \AA}$ ) and a graphite monochromator. The research was carried out by automatic step-by-step scanning in the  $U = 30 \text{ kV}$ ,  $I = 30 \text{ mA}$  mode in the interval of scattering angles from 3.0 to 80 degrees, exposure time 5 s.

Scherrer's formula was used to determine the size of the crystalline formations [21]:

$$L = \frac{k\lambda}{\beta \cos \theta_m}, \quad (1)$$

where  $\beta$  is the angular spread of the diffraction maximum (in radians), which is usually defined as full width at half maximum (FWHM) after preliminary subtraction of background scattering;  $k$  is a coefficient that depends on the crystallite (if the shape is not known, then  $k = 0.9$ );  $\theta_m$  is the angular position of the diffraction maximum.

The study of the temperature dependence of the heat flow was conducted in a dry air atmosphere of nitrogen in the temperature range from -100°C to 150°C at the heating rate of 10°C/min by differential scanning calorimetry (DSC) employing a DSC-60 Plus device (Shimadzu, Japan). The absolute error in determining the temperature of the phase and relaxation transitions was 0.1°C. The degree of crystallinity of the nanocomposites based on PU and AgNPs was calculated from the dependence of heat flow on temperature using the equation:

$$\chi_c = \frac{\Delta H_m}{\Delta H_{m,c}}, \quad (2)$$

where  $\Delta H_m$  is the measured melting enthalpy,  $\Delta H_{m,c}$  is the melting enthalpy of 100% crystalline polymer (for PTMG,  $\Delta H_{m,c} = 88 \text{ J/g}$  [22]).

The antimicrobial activity of the silver nanoparticles was studied by the method of diffusion in agar on a solid nutrient medium of Muller-Hinton for bacteria, and Sabouraud's medium for candida. Petri dishes with a nutrient medium were seeded with 10 $\mu$  L of inoculum of the test microorganisms *S. Aureus*, *E. coli* and *C. albicans* at the rate of 10<sup>8</sup> CFU/ml. After incubation for 24 hours at the temperature of 37°C, the width of the inhibition zone was measured. The antimicrobial activity of the nanocomposite coatings was studied by examining the development of colonies of microorganisms on the surface of the material. For this, a test culture of bacteria and fungi with a concentration of microorganisms equal to 10<sup>8</sup> CFU/ml was applied to the coating surface. After 48 hours of incubation at the temperature of 37°C, the number of live microorganisms in the inoculum on the surface of the synthesized nanocomposites was studied.

## RESULTS AND DISCUSSION

The distribution of nanofillers and their influence on the structure and properties of the polymer composite materials are largely determined by the method of manufacturing [13-18]. In this regard, two methods of introducing AgNPs developed by us into the composition of polymeric materials were proposed in this work. The segmented PU was used as a polymer component, which is technological in terms of production and the features of its structure are favorable for ensuring the strength and flexibility of such materials [23]. The first method is based on the combination of AgNPs as a colloidal solution in water with a solution of PU in DMF followed by the removal of solvents. This method is simple to perform, but limited by the solubility of the components: – the AgNPs developed by us are water-soluble and insoluble in DMF, while the solubility of PU is the opposite. Following this method, the composite materials with the designations PU-AgNPs(1:3)S and PU-AgNPs(1:9)S were obtained based on AgNPs(1:3) and AgNPs(1:9), respectively. The second method is based on the ultrasonic dispersion of the mentioned AgNPs in a solution of PU in DMF, followed by removal of the solvent. This method is not limited by the solubility of the individual components, but requires additional acoustic treatment. Following the second method, the composite materials PU-AgNPs(1:3)D and PU-AgNPs(1:9)D were obtained, respectively.

To establish the chemical structure of nanocomposite materials based on PU, the method of FTIR spectroscopy was used. The spectrum of the initial PU (Fig. 1, curve 1) is characterized by absorption bands  $\nu_{\text{sy}}$  C-O-C ( $1099\text{ cm}^{-1}$ ) and  $\nu_{\text{as}}$  C-O-C ( $1218, 1294\text{ cm}^{-1}$ ) of ether groups,  $\delta_{\text{sy}}$  C-H(CH<sub>3</sub>),  $\delta_{\text{as}}$  C-H(CH<sub>3</sub>),  $\delta$  C-H(CH<sub>2</sub>) ( $1407\text{ cm}^{-1}$ ) and  $\nu$  C-H(CH<sub>2</sub>, CH<sub>3</sub>), ( $2723, 2795, 2853, 2936\text{ cm}^{-1}$ ) of methyl and methylene groups,  $\nu_{\text{ar}}$  C-C ( $1400\text{-}1600\text{ cm}^{-1}$ ) of the aromatic component,  $\nu$  C-N ( $1367\text{ cm}^{-1}$ ),  $\delta$ N-H,  $\nu_{\text{sy}}$  N-C=O (amide (II)  $1512, 1535, 1562\text{ cm}^{-1}$ ),  $\nu$  NHC=O (amide (I)  $1637, 1691, 1730\text{ cm}^{-1}$ ) and  $\nu$  N-H ( $3283\text{ cm}^{-1}$ ) of the urethane and urea groups. The spectra of nanocomposites PU-AgNPs(1:3)D (curve 2), PU-AgNPs(1:9)D (curve 3) and PU-AgNPs(1:3)S (curve 4) are almost identical to this original PU (curve 1) as a consequence of the weak influence of the interaction of AgNPs with PU on the spectral characteristics of the composites at a given filler concentration. At the same time, significant changes are observed in the spectrum of the nanocomposite PU-AgNPs(1:9)D (curve 5) compared to the original PU, in particular, a slight hypsochromic shift of the absorption band  $\nu$  S=O, C-O-C of the original AgNPs is observed (from  $1020$  to  $1024\text{ cm}^{-1}$ , the FTIR-spectrum of AgNPs(1:9)), a significant change in the intensities of the absorption bands  $\nu_{\text{ar}}$  C-C ( $1400\text{-}1600\text{ cm}^{-1}$ ) of the aromatic component,  $\delta$ N-H,  $\nu_{\text{sy}}$  N-C=O (amide (II)  $1512, 1535, 1562\text{ cm}^{-1}$ ),  $\nu$  NHC=O (amide (I)  $1637, 1691, 1730\text{ cm}^{-1}$ ) and  $\nu$  N-H ( $3283\text{ cm}^{-1}$ ) of the ure-

thane and urea groups, as well as broadening of the last one. Such spectral changes indicate intensive interaction of AgNPs with the hard block of PU due to the interaction of ionic groups of the stabilizing shell of AgNPs with the urethane and urea groups of PU.

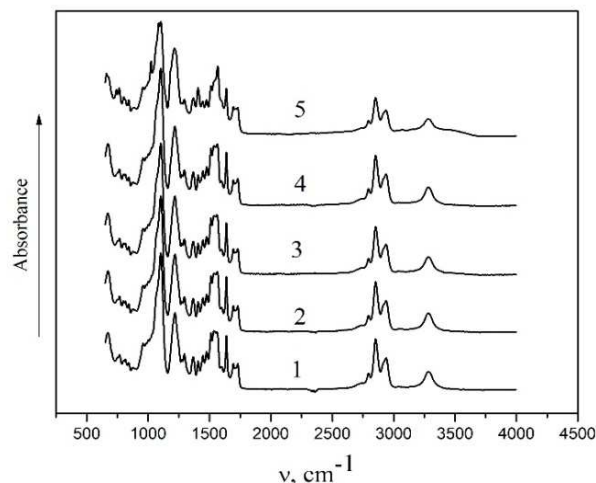


Fig. 1. FTIR spectra for unfilled PU (1) and nanocomposites PU-AgNPs(1:3)D (2), PU-AgNPs(1:9)D (3), PU-AgNPs(1:3)S (4) and PU-AgNPs(1:9)S (5)

The influence of the method of introducing the filler on the features of structure formation in PU-AgNP systems at a scale of up to 5 nm was studied by the method of wide-angle X-ray diffraction. Figure 2 shows the diffraction curves for the unfilled PU and PU-based nanocomposites containing different types of AgNPs introduced by different methods. For the unfilled PU, a very wide diffraction maximum is observed in the region of angles from  $13$  to  $30^\circ$  (Fig. 2, curve 1). It is known that PTMG, which is a part of PU, is a crystalline polymer, but its crystallinity significantly decreases during polymerization [24]. The reason for the significant decrease in the crystallinity of PTMG is its low molecular weight and the segmented structure of PU (the presence of flexible ether and hard urethane urea blocks). In particular, during the synthesis of PU, PTMG forms flexible oligoether blocks, and toluene diisocyanate in combination with 1,4-phenylenediamine forms hard urethane urea blocks prone to the formation of strong intermolecular bonds with the realization of a microphase-separated structure. The latter causes a significant decrease in the mobility of oligoether segments and, accordingly, their ability to form crystalline structures [25].

When AgNPs are introduced into the composition of the system, their diffraction curves change (Fig. 2, curves 2-5). A characteristic difference of the diffraction curves for nano-filled and unfilled PU is the presence of two diffraction peaks at  $38$  and  $45^\circ$ . These maxima indicate the presence of a silver crystal structure in the system and correspond to the (111) and (200) planes, respectively [26]. The low intensity of the diffraction peaks of silver, compared to the peak for

PTMG, is explained by the low contrast between the scattering of the matrix and the filler (2 wt.%).

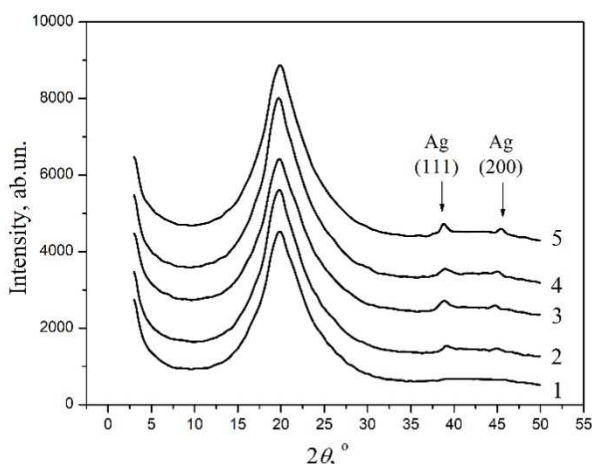


Fig. 2. Diffraction curves for unfilled PU (1) and PU-AgNPs(1:3)D (2), PU-AgNPs(1:3)S (3), PU-AgNPs(1:9)D (4) and PU-AgNPs(1:9)S (5) nanocomposites

Since PTMG, which is a part of PU, and synthesized silver nanoparticles have a crystalline structure, the effective crystallite size can be calculated for them. The half-width of the most intense maximum at  $38^\circ$  was used to calculate the effective size of the crystallites for the AgNPs introduced into the polymer matrix.

Table 1 shows the values of FWHM, the positions of the maxima, and the crystallite sizes calculated by Eq. (1) for PTMG and the introduced AgNPs.

TABLE 1. Values of diffraction peak parameters and calculated crystallite parameters for PTMG and Ag

Sample	PTMG crystals			Ag crystals		
	$\theta_m$ [°]	$\beta$ [°]	$L$ [nm]	$\theta_m$ [°]	$B$ [°]	$L$ [nm]
PU	20.09	5.53	1.44	–	–	–
PU-AgNPs(1:3)D	20.03	5.18	1.54	38.77	0.85	9.98
PU-AgNPs(1:3)S	20.08	5.60	1.42	38.75	0.83	10.00
PU-AgNPs(1:9)D	20.03	5.15	1.55	38.79	0.82	10.23
PU-AgNPs(1:9)S	20.07	5.41	1.47	38.78	0.80	10.29

Table 1 shows that during the formation of the PU matrix, the PTMG macromolecules form crystalline structures with an effective size of  $\sim 1.5$  nm. When different types of AgNPs are introduced into PU, the effective size of the PTMG crystallites changes within the measurement error. The method of filler introduction does not affect the effective size of the PTMG crystallites either.

By comparing the intensity and FWHM for the diffraction peaks, which are responsible for the structure of silver for systems containing AgNPs(1:3) and AgNPs(1:9), we can conclude that the method of introduction does not affect the effective size of the silver crystallites because AgNPs are formed before introduction into the polymer matrix.

The formation of silver nanoparticles of different sizes and the method of their introduction significantly affect the properties, in particular the thermophysical properties of the obtained PU-based materials. Figure 3 shows the results of DSC for the PU-based materials in the temperature range from  $-100$  to  $150^\circ\text{C}$ .

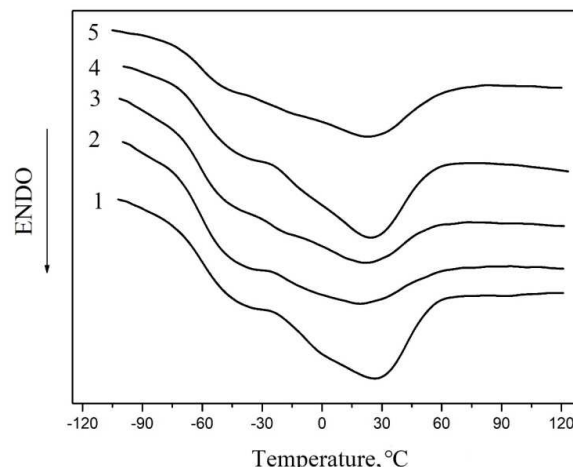


Fig. 3. DSC curves for unfilled PU (1) and PU-AgNPs(1:3)D (2), PU-AgNPs(1:3)S (3), PU-AgNPs(1:9)D (4) and PU-AgNPs(1:9)S (5) nanocomposites

Figure 3 shows that two temperature transitions are observed on the curves for all the studied systems: the glass transition, which occurs in the temperature range of  $-80$  to  $-30^\circ\text{C}$  and the melting process, in the interval from  $-30$  to  $60^\circ\text{C}$ . The main thermophysical characteristics for the studied materials are given in Table 2.

TABLE 2. Thermophysical characteristics of PU-based nanocomposite materials

	$T_g$ [°C]	$\Delta C_p$ [J/(g·°C)]	$T_m$ °C	$\Delta H_m$ [J/g]	X [%]
PU	-57.9	0.12	28.4	7.4	8.4
PU-AgNPs(1:3)D	-60.2	0.10	24.1	4.1	4.6
PU-AgNPs(1:3)S	-60.5	0.08	22.2	8.4	9.5
PU-AgNPs(1:9)D	-59.7	0.10	26.3	5.4	6.1
PU-AgNPs(1:9)S	-60.9	0.08	26.4	11.7	13.3

Figure 3 and Table 2 show that the introduction of AgNPs with different stabilizer contents significantly affects the final thermophysical properties of the obtained nanocomposites. The introduction of AgNPs leads to a decrease in the glass transition temperature of the polyurethane matrix, which is a typical effect of plasticization. At the same time, AgNPs reduce the cooperative mobility of PU macromolecules. A boundary layer of PU molecules is formed around the nanoparticles, which are sterically restricted and lose their mobility. This leads to a decrease in the share of PU polymer chains that are capable of glass transition, which is indicated by a decrease in the heat capacity jump during glass transition ( $\Delta C_p$ ) (Tab. 2).



Table 2 also shows that the method of introducing of nanoparticles affects the thermophysical characteristics of the composites. This effect is especially evident in the change of the  $\Delta C_p$  parameter. For systems in which nanoparticles were introduced from the solution, lower values of the  $\Delta C_p$  jump are observed compared to other systems. This effect indicates a more uniform distribution of filler particles, which results in an increase in the matrix-nanoparticle interaction surface. In the case of introducing nanoparticles by the dispersion method, the interaction surface of the matrix and nanoparticles becomes lower. That probably can be explained by the formation of aggregates, which reduces the total surface area of the filler.

AgNPs also affect the remains of the crystalline phase of PTMG, which is a part of PU. Thus, when nanoparticles are introduced by the dispersion method, the degree of crystallinity of the polymer matrix decreases from 8.4% for unfilled PU to 4.6% in the case of filling with AgNPs(1:3) and to 6.1% for systems with AgNPs(1:9). A decrease in the melting temperature of nanocomposites by 2-4°C compared to the unfilled matrix are also observed. Probably the PTMG crystals become smaller and more defective, which require less energy to melt. In the case of introducing nanoparticles from the solution, the degree of crystallinity increases to 9.5 and 11.3% for the systems containing AgNPs(1:3) and AgNPs(1:9), respectively. The effect of an increase in the degree of crystallinity is related to the nucleation effect of nanoparticles, which act as nucleation centers of the PTMG crystalline phase [27].

Comparing the influence of nanoparticles with a different stabilizer content on the thermophysical characteristics of the obtained materials, it can be concluded that smaller particles have a greater influence on the final properties.

As is known, silver nanoparticles have high antimicrobial activity. Therefore, the next stage of our work was the study of the inhibitory ability of polymer nanocomposite coatings that contained AgNPs.

Before studying the antimicrobial properties of polyurethane materials, the influence of the nanoparticles in powder form on gram-positive, gram-negative bacteria and mycotic flora was studied by the disk diffusion method. It was established that AgNPs exhibit a very high inhibitory capacity against *S. aureus*, *E. coli* and *C. albicans*. At the same time, for silver nanoparticles, the width of the inhibition zone for *S. aureus* was 30 mm, for *E. coli* – 12 mm, and for *C. albicans* – 34 mm.

To study the antimicrobial properties of the obtained nanocomposite polyurethane materials, the ability of the test cultures of microorganisms to form a biofilm at the boundary of the solid-gas phase was investigated. For this, a test culture of bacteria and fungi with a concentration of microorganisms equal to  $10^8$  CFU/ml was applied to the coating surface. After 48 hours of incubation, the number of live microorganisms in the inocu-

lum on the surface of the synthesized nanocomposites was studied. The results of the research are given in Table 3.

TABLE 3. Concentration of microorganisms in inoculum on surface of studied materials 48 hours after incubation

	<i>S. aureus</i> [CFU/ml]	<i>E. coli</i> [CFU/ml]	<i>C. albicans</i> [CFU/ml]
PU	$5 \cdot 10^7$	$8 \cdot 10^7$	$1 \cdot 10^7$
PU-AgNPs(1:3)D	$4 \cdot 10^5$	$7 \cdot 10^5$	$4 \cdot 10^4$
PU-AgNPs(1:3)S	$1 \cdot 10^5$	$4 \cdot 10^5$	$2 \cdot 10^4$
PU-AgNPs(1:9)D	$7 \cdot 10^5$	$2 \cdot 10^6$	$4 \cdot 10^4$
PU-AgNPs(1:9)S	$3 \cdot 10^5$	$8 \cdot 10^5$	$1 \cdot 10^4$

Table 3 shows that the synthesized nanocomposite materials exhibit antimicrobial properties. After incubation, active colonies of microorganisms remained on the surface of the unfilled PUs, the concentration of which decreased by 2-10 times, but remained at a sufficiently high level of about  $10^7$  CFU/ml. When the systems are filled with AgNPs(1:3), the concentration of all types of microbes is significantly reduced. Compared to the initial concentration of microorganisms equal to  $10^8$  CFU/ml, their concentration decreased by two decimal orders in the case of bacteria and by three orders in the case of mycotic flora. Similar effects of reducing the concentration of microorganisms on the surface were obtained for systems based on polyurethanes which contained silver nanoparticles stabilized with polyethylene glycol [28], as well as for materials based on polyethylene oxide and NPs [16]. The results for the PU-AgNPs(1:9) system occurred to be almost similar. The difference is slightly worse inhibitory activity against *E. coli* bacteria, which is explained by the larger size of silver nanoparticles in the system. In addition, Hung et al. demonstrated that the surface morphology has a major influence on the antimicrobial adhesion of PU-Ag nanocomposites [29]. In particular, they demonstrated that the smaller the characteristic size of the hard segments to which the hydrophilic Ag has a better affinity, the better the antibacterial activity. The method of introducing of nanoparticles has a weak effect. With the introduction of AgNPs from a solution, all the indicators of the antimicrobial activity of PU films occurred to be slightly higher than at the introduction of AgNPs by dispersion.

## CONCLUSIONS

As a result of the work, the effect of the method of introducing AgNPs into the segmented PU on the structure and properties of the resulting nanocomposites was determined. AgNPs were introduced into the PU matrix by the combination of a colloidal aqueous solution of AgNPs with a solution of PU in DMF or ultrasonic dispersion of nanoparticles in a solution of PU in DMF followed by the removal of solvents.

FTIR data provides evidence about the intense interaction of AgNPs with the PU hard block owing to the interaction of ionic groups of the stabilizing shell of AgNPs with the urethane and urea groups of PU only for the nanocomposite obtained by combining a solution of AgNP(1:3) in water and PU in DMF. For other materials, the lack of such spectral evidence is due to the weak influence of the interaction of AgNPs with PU on the FTIR spectra at a given filler concentration.

It was found that the method of introduction significantly affects the nature of crystalline phase formation in PU-AgNP systems. Thus, when nanoparticles are introduced by the dispersion method, crystallinity is suppressed, which is evidenced by a decrease in the effective size of PTMG crystallites and a decrease in the degree of crystallinity. For composites into which AgNPs were introduced from the solution, the opposite effect is observed: the formation of larger PTMG crystallites and growth of the crystalline phase are observed.

It was found that for systems in which nanoparticles were introduced from the solution, lower values of the heat capacity jump during glass transition are observed compared to other systems. This effect is explained by the smaller number of macromolecule structural elements capable of glassing, which can be a consequence of either a decrease in the volume of the amorphous phase as a whole or an increase in the number of immobilized macromolecules located in the boundary layer of a nanoparticle.

It has been shown that PU-AgNP composites exhibit very high inhibitory activity against *S. aureus*, *E. coli* and *C. albicans*. The concentration of all types of microbes is significantly reduced when the PU systems are filled. Compared to the initial concentration of microorganisms equal to  $10^8$  CFU/ml, their concentration decreased by two orders of magnitude in the case of bacteria and by three orders in the case of fungi. At the same time, the method of introducing nanoparticles has a weak effect. With the introduction of AgNPs from a solution, all the indicators of the antimicrobial activity of PU films occurred to be slightly higher than for the introduction of AgNPs by dispersion.

## Acknowledgements

*This work was carried out within the framework of the research project "Development of innovative technologies for the creation of silver-containing antimicrobial nanocomposite polymer materials with specified multifunctional characteristics for special purposes", which is financed from the state budget by the Ministry of Education and Science of Ukraine. State registration number 0122U002326.*

## REFERENCES

- [1] Hiremath A., Murthy A.A., Thipperudrappa S., Bharath K.N., Nanoparticles filled polymer nanocomposites: A technological review, *Cogent Engineering* 2021, 8, 1991229, DOI: 10.1080/23311916.2021.1991229.
- [2] Radhakrishnan S., Nagarajan S., Belaid H. et al., Fabrication of 3D printed antimicrobial polycaprolactone scaffolds for tissue engineering applications, *Materials Science and Engineering: C* 2021, 118, 111525, DOI: 10.1016/j.msec.2020.111525.
- [3] Lysenkov E., Klymenko L., Determination of the effect of carbon nanotubes on the microstructure and functional properties of polycarbonate-based polymer nanocomposite materials, *Eastern European Journal of Enterprise Technologies* 2021, 4(12), 112, 53-60. DOI: 10.15587/1729-4061.2021.239114.
- [4] Lan W., Li S., Shama S. et al., Investigation of ultrasonic treatment on physicochemical, structural and morphological properties of sodium alginate/AgNPs/Apple polyphenol films and its preservation effect on strawberry, *Polymers* 2020, 12, 2096, DOI: 10.3390/polym12092096.
- [5] Lysenkov E.A., Lysenkova I.P., Influence of nanodiamonds on the structure and thermophysical properties of polyethylene glycol-based systems, *Functional Materials* 2020, 27(4), 774-780, DOI: 10.15407/fm27.04.774.
- [6] González E.A., Leiva N., Vejar N. et al., Sol-gel coatings doped with encapsulated silver nanoparticles: inhibition of biocorrosion on 2024-T3 aluminum alloy promoted by *Pseudomonas aeruginosa*, *Journal of Materials Research and Technology* 2019, 8(2), 1809-1818, DOI: 10.1016/j.jmrt.2018.12.011.
- [7] Zhylytsova S.V., Leonova N.G., Lysenkov E.A., Klymenko L.P., Influence of 3-glycidoxypropyltriethoxysilane on the structural organization of epoxy-silica nanocomposites, *Theor. Exp. Chem.* 2021, 57, 154-161, DOI: 10.1007/s11237-021-09685-3.
- [8] Demchenko V., Shtompel' V., Riabov S., Lysenkov E., Constant electric and magnetic fields effect on the structuring and thermomechanical and thermophysical properties of nanocomposites formed from pectin-Cu<sup>2+</sup>-polyethyleneimine interpolyelectrolyte-metal complexes, *Nanoscale Research Letters* 2015, 10, 479, DOI: 10.1186/s11671-015-1181-z.
- [9] Vukoje I.D. et al., Characterization of silver/polystyrene nanocomposites prepared by in situ bulk radical polymerization. *Mater. Res. Bull.* 2014, 49, 434-439, DOI: 10.1016/j.materresbull.2013.09.029.
- [10] Qiu H., Si Z., Luo Y. et al., The Mechanisms and the applications of antibacterial polymers in surface modification on medical devices, *Front. Bioeng. Biotechnol.* 2020, 8, 910, DOI: 10.3389/fbioe.2020.00910.
- [11] Ahmad S.A., Das S.S., Khatoun A. et al., Bactericidal activity of silver nanoparticles: A mechanistic review, *Materials Science for Energy Technologies* 2020, 3, 756-769, DOI: 10.1016/j.mset.2020.09.002.
- [12] Mansoor S., Zahoor I., Baba T.R. et al., Fabrication of silver nanoparticles against fungal pathogens, *Front. Nanotechnol.* 2021, 3, 679358. DOI: 10.3389/fnano.2021.679358.
- [13] Zhang S., Tang Y., Vlahovic B., A Review on preparation and applications of silver-containing nanofibers, *Nanoscale Research Letters* 2016, 11, 80. DOI: 10.1186/s11671-016-1286-z.
- [14] Lyutakov O., Kalachyova Y., Solovyev A. et al., One-step preparation of antimicrobial silver nanoparticles in polymer matrix, *J. Nanopart. Res.* 2015, 17, 120, DOI: 10.1007/s11051-015-2935-3.
- [15] Demchenko V., Riabov S., Iurzhenko M., Rybalchenko N., A novel method for the formation of silver-containing nanocomposites-thermochemical reduction of Ag<sup>+</sup> ions in polymer films, [In:] Pogrebnjak A., Bondar O. (eds), *Microstruc-*

- ture and Properties of Micro- and Nanoscale Materials, Films, and Coatings (NAP 2019), Springer Proceedings in Physics, Springer, Singapore 2020, DOI: 10.1007/978-981-15-1742-6\_17.
- [16] Lysenkov E., Stryutsky O., Polovenko L., *Nanomaterials: Applications and Properties (IEEE NAP 2022): Proc. of 12th International Conference Nanomaterials: Applications and Properties (11-16 September 2022, Krakow, Poland)*, DOI: 10.1109/NAP55339.2022.9934675.
- [17] Qu R.J. et al., Preparation and property of polyurethane/nanosilver complex fibers, *Appl. Surf. Sci.* 2014, 294, 81-88, DOI: 10.1016/j.apsusc.2013.11.116.
- [18] Demchenko V., Mamunya Y., Kobylinskyi S. et al., Structure-morphology-antimicrobial and antiviral activity relationship in silver-containing nanocomposites based on polylactide, *Molecules* 2022, 27, 3769, DOI: 10.3390/molecules27123769.
- [19] Rivas L., Sanchez-Cortes S., Garcia-Ramos J.V. et al., Growth of Silver colloidal particles obtained by citrate reduction to increase the raman enhancement factor, *Langmuir* 2001, 17(3), 574-577, DOI: 10.1021/la001038s.
- [20] Shevchenko V.V., Stryutsky A.V., Klymenko N.S. et al., Protic and aprotic anionic oligomeric ionic liquids, *Polymer* 2014, 55(16), 3349-3359, DOI: 10.1016/j.polymer.2014.04.020.
- [21] Sun C.C., You A.H., Teo L.L., XRD measurement for particle size analysis of PMMA polymer electrolytes with SiO<sub>2</sub>, *International Journal of Technology* 2022, 13(6), 1336-1343, DOI: 10.14716/ijtech.v13i6.5927.
- [22] Xie H., Wu L., Li B.-G. et al., Poly(ethylene 2,5-furandicarboxylate-*mb*-poly(tetramethylene glycol)) multiblock copolymers: From high tough thermoplastics to elastomers, *Polymer* 2018, 155, 89-98, DOI: 10.1016/j.polymer.2018.09.033.
- [23] Korley L.T.J., Pate B.D., Thomas E.L., Hammond P.T., Effect of the degree of soft and hard segment ordering on the morphology and mechanical behavior of semicrystalline segmented polyurethanes, *Polymer* 2006, 47(9), 3073-3082, DOI: 10.1016/j.polymer.2006.02.093.
- [24] Luo K., Wang L., Chen X. et al., Biomimetic polyurethane 3D scaffolds based on polytetrahydrofuran glycol and polyethylene glycol for soft tissue engineering, *Polymers* 2020, 12, 2631. DOI: 10.3390/polym12112631.
- [25] Qin Z., Yunhui L., Kevin C.C., Surface biocompatible modification of polyurethane by entrapment of a macromolecular modifier, *Colloids Surf. B Biointerfaces* 2013, 102, 345-360. DOI: 10.1016/j.colsurfb.2012.07.037.
- [26] Meng Y., A Sustainable approach to fabricating Ag nanoparticles/PVA hybrid nanofiber and its catalytic activity, *Nanomaterials* 2015, 5, 1124-1135, DOI: 10.3390/nano5021124.
- [27] Wang Y., Lang X., Fan S. Accelerated nucleation of tetrahydrofuran (THF) hydrate in presence of ZIF-61, *Journal of Natural Gas Chemistry* 2012, 21(3), 299-301, DOI: 10.1016/S1003-9953(11)60367-8.
- [28] Mtimet I., Lecamp L., Kebir N. et al., Green synthesis process of a polyurethane-silver nanocomposite having biocide surfaces, *Polymer Journal* 2012, 44, 1230-1237, DOI: 10.1038/pj.2012.90.
- [29] Hung H.S., Hsu S.H., Biological performances of poly(ether)urethane-silver nanocomposites, *Nanotechnology*, 2007, 18, 475101-475110. DOI: 10.1088/0957-4484/18/47/475101.